Thermography-based assessment of mean radiant temperature and occupancy in healthcare facilities

Paul Seiwert[1], Quan Jin[2], Kai Rewitz[1], Ulrike Rahe[3], Dirk Müller[1]

1 RWTH Aachen University
Mathieustraße 10
52066 Aachen, Germany
**Corresponding author:pseiwert@eonerc.rwth-aachen.de*

2 Chalmers University of Technology
Chalmersplatsen 4
412 96 Gothenburg, Sweden

3 Hochschule Wismar
Philipp-Müller-Straße 14
23966 Wismar; Germany

ABSTRACT

Abstract. Due to its high demands regarding indoor environmental conditions, healthcare facilities are associated with high energy consumption. To move forward towards more demand driven and energy reduced conditioning, information on occupancy and temperature boundary conditions are crucial. Thermography-based systems enable data acquisition regarding both aspects in high local resolution. In this publication, we propose a thermography system that may be used for monitoring of rooms in healthcare facilities. It is set up using a 160 x 120 px thermography sensor and Raspberry Pi computer for data acquisition and processing. The sensors are mounted on walls to capture the inside of the room including patients, staff, and visitors. We evaluate the mean radiant temperature based on the individual inner surfaces of the room. The algorithm aggregates wall, floor and ceiling surface temperatures within the field of view of the sensor. For occupancy estimation inside the room, we apply a convolutional neural network (CNN). It is based on a pre-trained network and retrained using a partial dataset collected during the field study. To improve robustness of the algorithm several data pre-processing steps are conducted, that include image filters and redundancy testing. The system is evaluated based on data collected in a field study conducted inside MHH Hospital in Hannover, Germany. Several patients' rooms and a staff room are monitored over a period of 6 weeks, with the goal of evaluating indoor environmental data. The measurement period is inside the heating period in winter and different room layouts are considered. For reference, an indoor environmental quality measurement device is used to simultaneously measure air temperature, globe temperature and other IEQ parameters. Measured data of the reference system agree well with the thermography system. Deviations between both are less than 1 K in radiant temperature for most scenarios and measurement setups. Estimated occupancy is compared to a ground truth derived from manual processing of the captured thermography data. Finally, results of the field study are discussed together with the systems advantages and limitations with regard to privacy considerations.

KEYWORDS

Thermography, Occupancy detection, Mean radiant temperature, Computer Vision

1 INTRODUCTION

Continuous stress on the healthcare sector due to increasing life expectancy and threats from diseases has shifted public focus towards the conditions in healthcare facilities. Convalescence time and thus capacities in hospitals and other healthcare facilities are significantly influenced

by indoor environmental conditions (Shajahan et al., 2019). The high regulatory requirements for indoor conditions in these building types regarding ventilation rates and set temperatures, however, result in increased energy demand compared to other public buildings.

The methods and results presented within this publication are part of a pilot study to investigate measures for the improvement of well-being of patients and staff in hospitals as well as to convalescence and productivity. Furthermore, investigations into energy saving potentials are subject of the pilot study. It has been conducted between mid of November and mid of December 2020 in a ward of Medizinische Hochschule Hannover (MHH) and included both patients and staff's rooms.

Both the detection of occupancy and measurement of mean-radiant temperature (MRT) are crucial factors for efficient control of building energy systems. We propose a thermography-based system that enables the assessment of both aspects within one system.

1.1 Occupancy detection

During regular building operation indoor environmental conditions in healthcare facilities are typically not monitored under consideration of real-time occupancy. However, demand-controlled ventilation (DCV) enabled by occupancy detection can contribute to a significant decrease in heating, ventilation and air-conditioning (HVAC) related energy consumption in hospitals (Čongradac et al., 2014; Rätz et al., 2020).

For occupancy detection in indoor rooms several technologies have been proposed and investigated (Liu et al., 2019; Ahmad et al., 2021) In many applications, Pyroelectric Infrared Sensors (PIR) are used to detect presence of people, but they are not capable to retrieve information on the number of occupants. Derivation of occupancy from CO_2 measurements allows inexpensive and non-invasive detection, however with drawbacks in terms of accuracy, which can be improved with additional sensors in fusion with the CO_2 sensor (Dedesko et al., 2015; Rätz et al., 2022). Camera-based systems using machine learning algorithms are another option with high accuracy, but are sensitive with regards to the occupants' privacy.

Long-wave infrared (IR) sensors for occupancy detection are applied in different resolution and positions within indoor environments (Tyndall et al., 2016; Zhao et al., 2018). Analogous to camera-based systems, machine-learning algorithms are applied for classification based on the thermographic image. In most indoor conditions the high temperature difference between background and skin/clothing surface yields a good contrast for detection. The sensors can operate independent of illumination of the room and have become economically more viable. In terms of privacy, IR sensors are less critical as their lower resolution reveals less distinct features and less contrast than conventional cameras. Technical solutions for privacy implications have already been discussed (Pittaluga et al., 2016; Ahmad et al., 2021; Dubail et al., 2022).

1.2 Mean radiant temperature

According to ASHRAE standard 55 mean radiant temperature is – besides air temperature, air humidity and air speed – a required parameter to predict thermal comfort in thermal environments (ASHRAE, 2020). It is a key parameter for the quantification of radiative heat transfer between a person and its surrounding surfaces and is usually measured by means of a

globe temperature sensor, air temperature sensor and air velocity sensor. Further measurement methods include the two-sphere radiometer and the constant air temperature sensor (International Standardization Organization, 2002). As the radiative heat transfer is influenced by many factors including wavelength of radiation, view factors between objects and their surface temperature, its precise measurement is challenging, and it is associated with a high measurement uncertainty.

IR sensors allow continuous, non-intrusive measurement of surface temperatures. Using these measured surface temperatures and the view factors between the evaluation position and the surroundings, mean radiant temperature can be calculated analytically.

2 METHODS

2.1 Experimental setup and data acquisition

The experimental study is conducted as a field study within 5 different rooms of MHH: 4 patient rooms and 1 physicians' room. The rooms are equipped with mechanical ventilation systems and radiators for heating. Windows can be opened to allow for hybrid ventilation. In each of those rooms both IR sensor systems and an indoor environmental quality (IEQ) sensor system are installed.

Table 1: List of rooms with usage type and window orientation

Room	Type of room	Window Orientation	Number of beds
R1	Physicians room	North	-
R2	Patient room	North	2
R3	Patient room	South	2
R4	Patient room	South	3
R5	Patient room	South	2

The IR sensor system consists of a FLIR Lepton 3.5 160x120 px microbolometer sensor, the corresponding evaluation board for radiometric determination of object temperatures and a Raspberry Pi 3B+ microcomputer for data processing and transmission to storage. The sensor is specified with a typical accuracy of ±5 K within regular operating conditions in buildings. In each room 2 of these sensors have been installed in opposing upper corners of the rooms, facing towards the occupied zone of the room, to cover as much wall, ceiling, and floor surface area as possible with the field of view (FOV) of the sensors. The low FOV angle of 57/71° (horizontal/diagonal) compared to many other sensors limits the covered surface to mainly wall and floor sections.

The IEQ sensor system is used as a reference for the mean radiant temperature. The BAPPU-evo sensor device features among others air temperature (± 0.5 K), air humidity (± 4 % rH) and a globe temperature sensor (± 0.5 K). Due to restrictions regarding interference with care operations, the sensor system had to be placed on shelves slightly above the occupied zone at 2 m height.

In Figure 1 the positions of one of the IR sensor systems in a patient's room and one of the IEQ measurements systems are indicated.

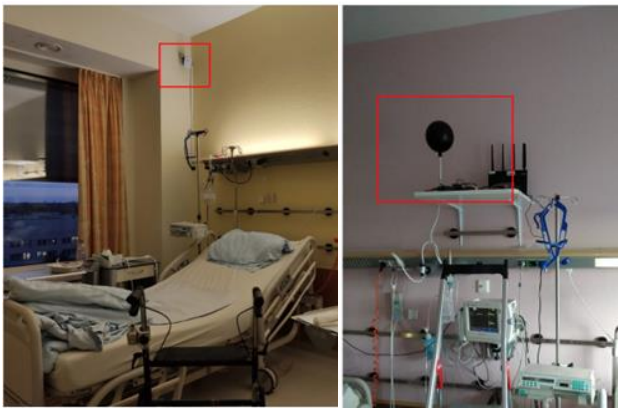

Figure 1: Positions of IR sensor system (left) and IEQ measurement system (right) inside a patient's room

2.2 Data pre-processing

The IR sensor system records frames with a frequency of 10 seconds. The frames are temporarily stored locally. In pre-processing the frame is analysed regarding its redundancy and validity. For redundancy testing the frame is compared to the previous frame based on the structural similarity index. In case the structural similarity is higher than 97% the frame is discarded. Occasionally, the sensor provides corrupted images which are detected based on a histogram comparison between frames. The frames are normalized and saved on a server in batches of 30 frames for further processing.

2.3 Occupancy

2.3.1 Data pipeline

The normalized frames are annotated manually by creation of labels for each occupant inside a room as shown in Figure 2. We have used one class of labels which includes occupants in different postures. These are standing, sitting, and lying. The images and annotations are saved and converted to the tfrecords format for further processing with machine learning platform TensorFlow (TensorFlow Developers, 2022).

Figure 2: Label annotations for occupants in patients' room

2.3.2 Network training

The TensorFlow platform provides pre-trained network architectures, which can be used for further individualized training of networks. The models suited for detection purposes are pre-

trained on the COCO 2017 dataset, which features images in the visual domain (Lin et al., 2014). We have selected the Faster R-CNN Inception ResNet V2 640x640 architecture (Szegedy et al., 2016). It is a very deep convolutional neural network with a good trade-off between accuracy and computational speed/ memory requirements. As the present frames are in the long-wave IR domain, the training process is cross-domain.

For transfer learning, we use a dataset of 800 frames, compiled randomly from 9 of the IR sensor systems. Data from one IR sensor system have been excluded due to faulty data. The network is trained in 100 000 steps with a batch size of 1. The development of the total loss metric for network training is shown in Figure 3. It includes classification loss, localization and objectness loss.

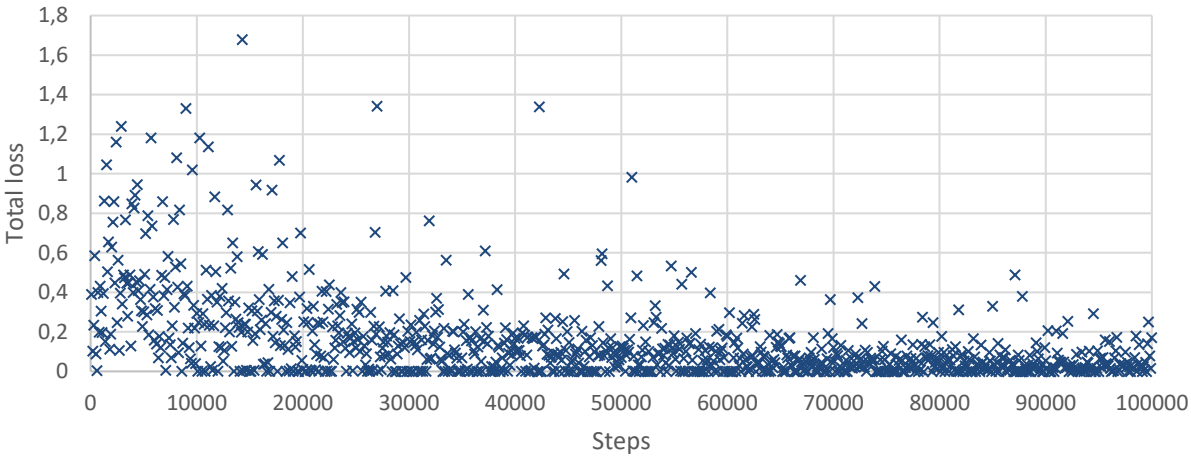

Figure 3: Total loss of network training process for each step

2.3.3 Training evaluation

For the evaluation of the networks training performance, COCO detection metrics are used. The confidence scores predicted by the classifier represent the probability that a bounding box contains a person. Precision indicates the reliability of the network's positive prediction, whereas recall describes the ability to determine the relevancy of predictions. The average precision is the average of precision values for all different levels of recall. The Intersection over Union (IoU) value represents the ratio of intersection area and union area of a predicted boundary box and a ground truth bounding box. The mean average precision (mAP) is calculated over different levels of IoU. The evaluation is based on an evaluation dataset of 200 frames from different sensor systems.

2.4 Mean radiant temperature

2.4.1 Algorithm for calculation

To determine MRT analytically both the surface temperatures t_i and view factors between the evaluation position and the surfaces F_{p-i} have to be known. According to ISO 7226 the following equation applies for the calculation of MRT indoor environments assuming high emissivity surfaces:

$$MRT^4 = \sum_{i=1}^{N} t_i^4 \cdot F_{p-i} \quad (1)$$

For small temperature differences, which are typical for surfaces in indoor environments it can be simplified to a linear equation:

$$MRT = \sum_{i=1}^{N} t_i \cdot F_{p-i} \quad (2)$$

The indoor surfaces temperature can be determined with the data captured by the IR sensor system. The surfaces are separated into segments based on their material properties, especially their emissivity. The assignment is done manually for the static position of the sensor after installation. For simplification of view factors, we substitute the view factors by arithmetic weighting according to the surface area A_i of each segment as shown in equation 3. This approach does not account for individual positions inside the room.

$$F_{p-i} = \frac{A_i}{\sum_{i=1}^{N} A_i} \quad (3)$$

Each surface is captured with one of the systems inside the rooms. The low angle of incidence between the sensor and ceiling results in a high share of reflected radiation. For this reason, the ceiling is not further considered for calculation. The expected error from this simplification is low for standing occupants, as projection factors according to ISO 7726 are small for ceiling and floor, compared to those for walls. However, for occupants in recumbent body position the expected error becomes more significant as the projection factor increases. An exemplary surface segmentation for a patient's room is shown in Figure 4.

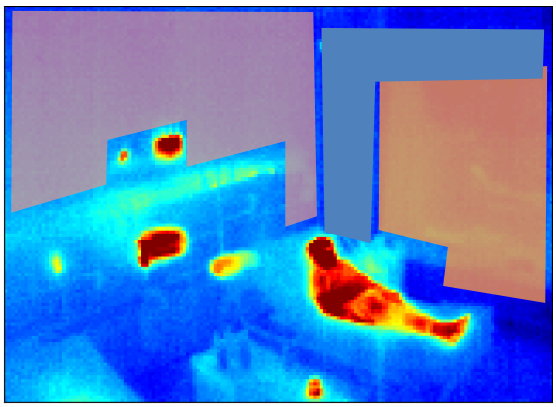

Figure 4: Exemplary selection of surfaces for MRT calculation for Room 4

After calculation of MRT, we filter not plausible outlier data by an Hampel-filter-function (based on a moving median) of MATLAB R2021a for a duration of five minutes. To reduce the noise of the sensor signals and to account for partial obstructions of surfaces by moving people, we finally calculated the moving mean value over five minutes for the data.
As a reference for the MRT, the globe temperature data from the IEQ measurement system are used. According to ISO 7226, MRT can be calculated from globe temperature t_g for forced convection based on equation 4, with air velocity v_a and air temperature t_a.

$$MRT = \left[\left(t_g + 273\right)^4 + 2.5 \cdot 10^8 \cdot v_a^{0.6} \times \left(t_g - t_a\right)\right]^{1/4} - 273 \quad (4)$$

The estimated deviation boundaries between globe temperature and calculated mean radiant temperature according to ISO 7226 are less than 0.8 K based on measured differences between air temperature and globe temperature of less than 2 K and air velocities of < 0.05 m/s.

3 RESULTS

3.1 Occupancy

In Figure 5 six exemplary frames from 4 different sensor systems with predicted boundary boxes are depicted. The green boundary boxes show the predicted position and area. The confidence scores at the top of the boundary boxes indicate the classifier confidence of the prediction being true.

In the top left frame both predictions are true positives. Also in the top right, bottom left and bottom center frame the predictions are correct. However, in the top right frame the IoU is lower than for the other predictions as only a part intersects with the ground truth (marked in red). In the top center frame the person lying in the bed is not detected (false negative) and in the bottom right frame a person is predicted, where nobody is present (false positive) indicating overfitting of the model.

The mean average precision (mAP) of the network for the evaluation data set is 0.4679 compared to the 0.377 of the pre-trained network on the COCO dataset. For an IoU of 0.5 the mAP significantly increases to 0.8028. For an IoU of 0.75 it is 0.4753. This means that the position of boundary boxes can be predicted well, but the intersection with annotated boundary box is not high for all cases as can be seen in the top right frame.

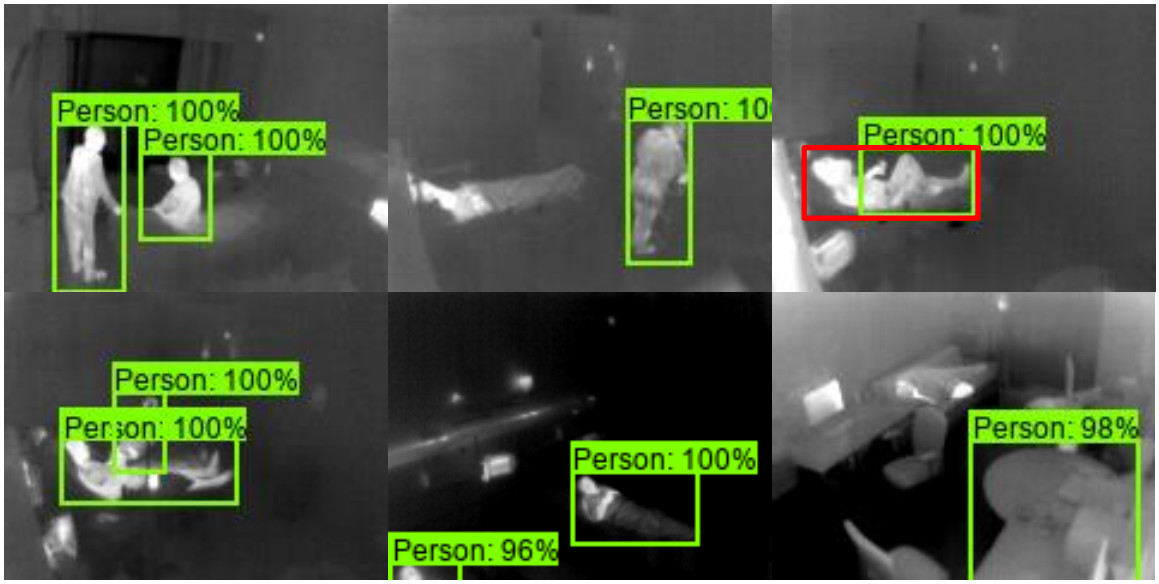

Figure 5: Selected frames of evaluation data set with predicted boundary boxes for persons marked in green

3.2 Mean radiant temperature

In Figure 6 the calculated MRT, air temperature and globe temperature as reference are depicted for Room 2 over the course of 18 days. Daily variations occur for the temperature profiles with

highest temperatures typically in the afternoon. A general trend with increasing temperatures from the beginning of the measurement period till the end can be observed.

Overall, the calculated MRT follows the globe temperature with little deviations. While in the beginning the difference between both values is continuously < 0.5 K, the difference increases after December 9th but stays within < 1 K. The RMSE between the MRT and the globe temperature for the whole measurement period in this room is 0.47 K.
Occasionally, short time temperature peaks occur for only one of the variables. For example, on December 5th the increase in globe temperature is significantly higher than for the MRT. A contrary effect can be observed on December 8th. Similar characteristics and effects can be observed for other rooms as well.

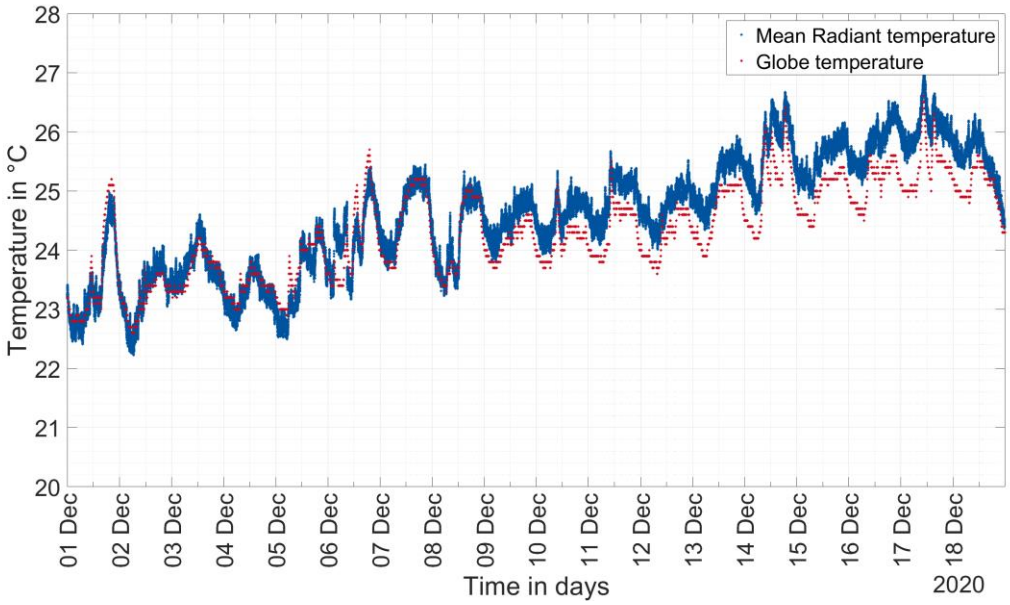

Figure 6: Calculated mean radiant temperature and measured globe temperature for Room 2

4 DISCUSSION

In terms of occupancy detection, the trained network yields good results for an estimation of occupancy in the rooms. In all different body postures, persons are detected by the network, although some predicted boundary boxes have a low IoU with the annotated boundary box. False negatives occur most frequently when the contrast between the person and the background is too low. High room temperatures lead to low differences between human skin or clothing temperature and the room temperature and thus lower contrasts, as we used normalized frames based on fixed temperature limits. Dynamic temperature limits may be a solution here, however implications for network training need to be considered as well.

As the pre-trained network was trained on visual domain images, features for classification are different in the frames used for further training and evaluation. Overfitting issues especially for specific sensor installation point may be caused by the low number of different installation points and fixed sitting and standing positions of patients and staff. Further classes (e.g. differentiation between postures) as well as more training data with different installation positions could reduce these issues.

Regarding privacy, the chosen installation position, sensor resolution and distance between sensor and person prevent direct identification of people as facial features are not recognisable. However, with further contextual information identification might be possible and technical

solutions must be implemented to reduce the associated concerns. Local data processing on the device and transfer of non-sensitive data to central building control systems can be part of the solution.

For the presented experimental setup, the applied calculation method for MRT shows only minor deviations compared to the reference globe temperature measurement and can therefore be considered valid. The homogenous boundary conditions comply with the assumptions made for the application of the method concerning view factors and temperature differences. As pointed out in the results section, some influencing and noise factors may have more significant impacts on the calculation methods which leads to limitations with regards to accuracy. These include ambient conditions such as air temperature and velocity but also body positions of occupants and distances between surfaces and evaluation positions. Further comfort relevant parameters such as radiation asymmetry and vertical temperature gradient may also be predicted based on the recorded data and could further enhance the capabilities of the system (Seiwert et al., 2018).

5 CONCLUSION

An IR sensor-based measurement system for occupancy detection and determination of mean radiant temperature has been presented in this work. The developed methodologies rely on image-based evaluation of data and comparison with measurements and manually annotated occupancy information.
For both aspects the results of the pilot study show promising results. The trained network can detect occupants inside the rooms with good precision and enables not only binary detection of occupancy but also a count of occupants. With further development and networks, which are exclusively trained on IR domain data, precision and recall may be further improved and model overfitting reduced. Privacy preserving algorithms can be implemented directly on the sensor system to reduce associated concerns.

With the calculation of mean radiant temperature, thermal boundary conditions inside rooms can be evaluated more accurately. The deviations measured in the observed rooms are within an acceptable range given the generally high uncertainty associated with its determination. Requirements regarding the boundary conditions have been fulfilled in this study, however they limit transferability to similar environments and require further validation.

6 ACKNOWLEDGEMENTS

We thank Tobias Schilling, Katharina Band and Iman El-Sayed from Medizinische Hochschule Hannover for their contribution in the preparation and conduction of the field study. Furthermore, we thank HeinzTrox Wissenschafts gGmbH and the Swedish Energy Agency for financial support of the study.

7 REFERENCES

Ahmad, J., Larijani, H., Emmanuel, R., Mannion, M. and Javed, A. (2021). Occupancy detection in non-residential buildings – A survey and novel privacy preserved occupancy monitoring solution. *Applied Computing and Informatics*, *17*(2), 279–295.

ASHRAE (2020). Standard 55-2020: Thermal Environmental Conditions for Human Occupancy.

Čongradac, V., Prebiračević, B. and Petrovački, N. (2014). Methods for assessing energy savings in hospitals using various control techniques. *Energy and Buildings*, *69*, 85–92.

Dedesko, S., Stephens, B., Gilbert, J.A. and Siegel, J.A. (2015). Methods to assess human occupancy and occupant activity in hospital patient rooms. *Building and Environment*, *90*, 136–145.

Dubail, T., Peña, F.A.G., Medeiros, H.R., Aminbeidokhti, M., Granger, E. and Pedersoli, M. (2022). Privacy-Preserving Person Detection Using Low-Resolution Infrared Cameras. https://arxiv.org/pdf/2209.11335.

International Standardization Organization (2002). ISO 7726:2002: Ergonomics of the Thermal Environment - Instruments for Measuring Physical Quantities. Geneva.

Lin, T.-Y., Maire, M., Belongie, S., Bourdev, L., Girshick, R., Hays, J., Perona, P., Ramanan, D., Zitnick, C.L. and Dollár, P. (2014). *Microsoft COCO: Common Objects in Context*.

Liu, J., Luo, H. and Zhang, W. (2019). An Overview of Real-time Occupancy Information Acquisition Method for Demand-driven Building Energy Management. In: Hajdu, M. (ed.), *Proceedings of the Creative Construction Conference 2019*: *29 June-2 July 2019, Budapest, Hungary*. Budapest: Budapest University of Technology and Economics; Diamond Congress Ltd, 625–634.

Pittaluga, F., Zivkovic, A. and Koppal, S.J. (2016). Sensor-level privacy for thermal cameras, *2016 IEEE International Conference on Computational Photography (ICCP)*: *Evanston, Illinois, 13-15 May 2016 : proceedings*. Piscataway, NJ: IEEE, 1–12.

Rätz, M., Kalliomäki, P., Mathis, P., Koskela, H. and Müller, D. (2020). Analyzing the Energy-Saving Potential of Demand-Controlled Ventilation in Hospitals via Dynamic Building Simulations, 1026–1031.

Rätz, M., Koskela, H., Kalliomäki, P., Müller, D. and Kremer, M.T. (2022). Real-Time Occupancy Detection in Hospital Patient Rooms Using Sensor Fusion, *Ventilation 2022: 13th International Industrial Ventilation Conference for Contaminant Control*.

Seiwert, P., Schmitt, L., Wesseling, M.T. and Müller, D. (2018). Detection of Vertical Air Temperature Distribution by Long-Wave Infrared Thermography. In: Finnish Society of Indoor Air Quality and Climate (ed.), *Proceedings: Roomvent&Ventilation 2018*: *Excellent Indoor Climate and High Performing Ventilation*. Helsinki, Finland: SIY Indoor Air Information Oy.

Shajahan, A., Culp, C.H. and Williamson, B. (2019). Effects of indoor environmental parameters related to building heating, ventilation, and air conditioning systems on patients' medical outcomes: A review of scientific research on hospital buildings. *Indoor Air*, *29*(2), 161–176.

Szegedy, C., Ioffe, S., Vanhoucke, V. and Alemi, A. (2016). Inception-v4, Inception-ResNet and the Impact of Residual Connections on Learning. arXiv. https://arxiv.org/pdf/1602.07261.

TensorFlow Developers (2022). *TensorFlow*. Zenodo.

Tyndall, A., Cardell-Oliver, R. and Keating, A. (2016). Occupancy Estimation Using a Low-Pixel Count Thermal Imager. *IEEE Sensors Journal*, *16*(10), 3784–3791.

Zhao, H., Hua, Q., Chen, H.-B., Ye, Y., Wang, H., Tan, S.X.-D. and Tlelo-Cuautle, E. (2018). Thermal-Sensor-Based Occupancy Detection for Smart Buildings Using Machine-Learning Methods. *ACM Transactions on Design Automation of Electronic Systems*, *23*(4), 1–21.